Jian-Lian Chen
Yi-Chen Lin

School of Pharmacy, China Medical University, Taichung, Taiwan

Received August 28, 2010
Revised September 28, 2010
Accepted September 28, 2010

Research Article

The role of methacrylate polymerized as porous-layered and nanoparticle-bound phases for open-tubular capillary electrochromatography: Substitution of a charged monomer for a bulk monomer

The bulk monomer, butyl methacrylate (BMA), was copolymerized with an ionizable monomer (mono-(2-(methacryloyloxy)ethyl) succinate (MES)) and carbon nanotubes (CNTs) by ethylene dimethacrylate (EDMA) crosslinking to form the porous-layered and nanoparticle-bound stationary phases for open-tubular CEC. Here, two new phases were synthesized to check the role of BMA on the BMA-MES and BMA-CNT phases and the suitability of the MES monomer for concurrently acting as a bulk monomer. One phase, MES-EDMA, was simply composed of MES monomer and EDMA crosslinker and exhibited a phase construction of molecular layers, in contrast to the polymeric phases of BMA-MES. Another phase studied was MES-CNT, which SEM images showed that MES could be a good bulk monomer for a CNT-polyacrylate composite phase with embedded CNTs. For all the modified capillaries, the EOF profiles observed in phosphate buffers between pH 3.6 and 9.6 were comparable with each other and conformed to their corresponding SEM images. The residual silanols retained their influence on the EOF profiles in the MES-EDMA and BMA-MES capillaries, but diminished in the CNT-bound capillaries. In a comparison with the MES-EDMA capillary, the BMA-MES capillary afforded a stronger interaction with flavonoids and phenolic acids and still retained positive capacity factor values. Additionally, the capacity factors obtained from the BMA-CNT capillary were higher than those from the MES-CNT capillary, as the BMA-CNT phase had hydrophobic BMA units and a high surface contact area of bound CNTs.

Keywords:
CEC / Multi-wall carbon nanotube / Particle-bound / Polyacrylate / Stationary phases
DOI 10.1002/elps.201000436

1 Introduction

Since Hjertén first reported the preparation of polyacrylamide as a continuous polymer bed in 1989 [1], the development of organic polymer phases for microscale chromatographic separations, including CEC, capillary LC, and microfluidic devices, has been remarkable [2–5]. For CEC, this development leads the advancements in column technology for its ease of fabrication, versatile surface modifications, higher permeability, and good peak capacity. Additionally, the CEC performance of the polymer-based phases, including monolith, molecularly imprinted polymers, open-tubular (OT), and particle-bound columns, is greatly influenced by the polymer characteristics. In comparison with OT and particle-bounded formats, monolith and molecularly imprinted polymers have been more extensively investigated in regards to the optimization of their *in situ* polymerization parameters [6, 7].

Among the three major categories of monoliths (acrylate/methacrylate-, acrylamide-, and styrene-based), the acrylate/methacrylate type is the most popular as the size and distribution of the pores on the phase surfaces for this type were determined by initiators and porogenic solvents [8–11]. Furthermore, a ternary cross-linker, trimethylolpropane trimethacrylate, was compared with the binary ethylene dimethacrylate (EDMA) in ternary porogen mixtures [12]. Variations in the ratio of bulk monomer to porogen and the kinds of bulk monomer used in the synthetic conditions

Correspondence: Dr. Jian-Lian Chen, School of Pharmacy, China Medical University, No.91 Hsueh-Shih Road, Taichung 40402, Taiwan
E-mail: cjl@mail.cmu.edu.tw
Fax: +886-4-22031075

Abbreviations: **BMA,** butylmethacrylate; **CNT,** carbon nanotube; **EDMA,** ethylene dimethacrylate; **γ-MAPS,** 3-(trimethoxysilyl) propylmethacrylate; **MeOH,** methanol; **MES,** mono-(2-(methacryloyloxy)ethyl) succinate; **MWNT,** multi-walled carbon nanotube; **OT,** open-tubular

were also shown to have a significant impact on the phase morphology and the electrochromatographic performance of the supports [13–16]. Besides, some ionizable methacrylate monomers are incorporated in the monolithic phases for specific functionality, such as ion exchangers, chiral selectors, and protein affinity, besides simply resulting in electric double layers and providing EOF [17–20]. However, no evidence has yet proven an ionizable monomer to be unsuitable for concurrently acting as a bulk monomer.

Although OT-CEC columns draw less attention than monolithic columns due to their lack of phase ratios, the OT column is a comparatively straightforward style that does not require the blending of constituent monomers with suitable porogens in precise proportions, which is typical for the generation of monoliths that are not plugged and that have well-distributed pores [2, 5, 21, 22]. By contrast, it is easy to leave a certain thickness of polymer film on an OT capillary for initial studies of new stationary phases. In this manner, some research has shown the separation of various analytes on styrene-based [23, 24] and acrylate-based [25–33] OT-CEC columns. In regards to the particle-bound polymer phases, they were mostly found in monolithic columns [34–36], but their use in an OT fashion was only investigated in a carbon nanotubes (CNTs)-bound polyacrylate [37].

Mono-2-(methacryloyloxy)ethyl succinate (MES) is an ionizable acrylate monomer that is newer than the commonly used monomers, such as 2-acrylamido-2-methylpropanesulfonic acid and 2-[2-(methacryloxy)ethyl] trimethylammonium. In our previous studies on OT-CEC, butyl methacrylate (BMA) was successfully copolymerized with MES monomer and CNTs to produce the porous-layered (BMA-MES) and CNTs-bound (BMA-CNT) phases, respectively [33, 37]. In this study, two new phases were formed to check the role of BMA on the two previous phases and the suitability of the MES monomer to concurrently act as a bulk monomer. One phase was synthesized by the removal of BMA from the *in situ* BMA-MES polymerization solution, and another by the replacement of BMA for the MES monomer in the *in situ* BMA-CNT polymerization solution. After characterization of the completed capillaries by EOF measurements and SEM, the new columns were used to separate flavonoids and phenolic acids and the resulting electrochromatographic performance and parameters were compared with previously obtained data.

2 Materials and methods

2.1 Reagents and chemicals

Most chemicals used were of analytical or chromatographic grade. Purified water (18 MΩ cm) from a Milli-Q water purification system (Millipore, Bedford, MA, USA) was used to prepare samples and buffer solutions. MES ($H_2C = C(CH_3)CO_2CH_2CH_2O_2CCH_2CH_2CO_2H$), EDMA, 2,2-diphenyl-1-picrylhydrazyl, AIBN, 1,4-butanediol, nine flavonoids (5-methoxyflavone, hesperidin, naringin, catechin, epicatechin, hesperetin, daidzein, naringenin, and quercetin), five phenolic acids (chlorogenic, *p*-coumaric, gallic, ferulic, and protocatechuic acids), and ethylvanillin were purchased from Aldrich (Sigma-Aldrich, Milwaukee, WI, USA). 3-(Trimethoxysilyl) propylmethacrylate (γ-MAPS), syringic acid, and vanillic acid were purchased from Acros (Thermo Fisher Scientific, Geel, Belgium). Boric acid, trisodium phosphate, methanol (MeOH), acetone, and ethanol were obtained from Panreac (Barcelona, Spain). BMA, *p*-hydroxybenzoic acid, ACN, DMSO, 1-propanol, hydrochloric acid, phosphoric acid, nitric acid, sodium hydroxide, sodium dihydrogenphosphate, disodium hydrogen phosphate, trisodium phosphate, and sodium tetraborate were supplied by Merck KGaA (Garmstadt, Germany).

The multi-walled carbon nanotube (MWNT) material was supplied by Conyuan Biochemical Technology (Taipei, Taiwan) and their specifications were 20–40 nm external diameter, 5–15 m length, 95–98% purity by volume, 40–300 m^2/g for the special surface area, 2 wt% amorphous carbon, and 0.2 wt% ash.

To make stock solutions, flavonoids were dissolved in MeOH (0.25 mg/mL) and phenolic acids were dissolved in H_2O (0.1 M). All solvents and buffer solutions for CEC analysis were filtered through a 0.45-μm cellulose ester membrane (Adventec MFS, Pleasanton, CA, USA).

2.2 Apparatus

The laboratory-built electrophoresis apparatus consisted of a ±30 kV high-voltage power supply (TriSep TM-2100, Unimicro Technologies, CA, USA) and a UV-Vis detector (LCD 2083.2 CE, ECOM, Prague, Czech Republic). Electropherograms were recorded using a Peak-ABC Chromatography Data Handling System (Kingtech Scientific, Taiwan). The SEM images were acquired at an accelerating voltage of 3.0 kV using a Joel JSM-6700F Scanning Microscope at National Chung Hsing University, Taiwan.

2.3 Preparation of capillary columns

Through silanization with the γ-MAPS reagent, the capillary silica surface was modified with acrylate bridging ligands, and the silanized surface was prepared for subsequent attachment of the acrylate polymer to the inner wall of the capillary following *in situ* polymerization. The synthesis of BMA-MES and BMA-CNT capillaries has been reported previously [33, 37]. Two types of capillaries, MES-EDMA and MES-CNT, had to be prepared in this study and their preparation procedures, including column pretreatment, cleaning, and silanization, were identical to the previous reported methods, but various recipes were sued in the preparation of the polymerization solution. The polymerization solution prepared for the MES-EDMA capillary was similar to that for the BMA-MES capillary, but lacked the

BMA monomer in the mixture. For the MES-CNT capillary, the MES monomer was substituted for the BMA monomer in the polymerization solution prepared for the BMA-CNT capillary.

The steps before coating a polymerization solution are described as follows: a new, bare 375 μm od × 75 μm id capillary column (Polymicro Technologies, Phoenix, AZ, USA) was treated with 1.0 M NaOH at 120°C for 2 h to increase the silanol density. The treated column was then cleaned by flushing with pure water, 1.0 M HCl, pure water, and acetone, in that order. After flushing, the clean capillary was filled with a solution of 2,2-diphenyl-1-picrylhydrazyl (0.02 g), γ-MAPS (1.0 mL), and MeOH (1.0 mL) and was then kept at room temperature for 24 h. Following a series of rinses with MeOH, H_2O, and acetone, the resulting silanized capillary was available for filling with the polymerization solution.

For the MES-EDMA capillary, the silanized capillary was filled with the polymerization solution, which contained MES monomer (0.01 mol), EDMA (0.01 mol), AIBN (0.3 g), 1-propanol (13.5 mL), 1,4-butanediol (13.5 mL), and H_2O (3 mL). After standing for 1 h at ambient temperature, the mixture was purged *via* the application of a nitrogen flow at 30 psi for 1 h to leave a thin layer of monomer materials ready to react with the silanized capillary.

For the MES-CNT capillary, its polymerization solution was comprised of MES monomer (0.03 mol), EDMA (0.01 mol), acid-treated MWNTs (1 mg), AIBN (0.1 g), 1-propanol (4.5 mL), 1,4-butanediol (4.5 mL), and H_2O (1 mL). The acid-treated MWNTs were obtained by first refluxing the MWNTs with HNO_3 (3.0 M) for 24 h at 60°C and then with HCl (5.0 M) for 6 h at 120°C. After standing for 1 h at ambient temperature, the mixture was purged *via* the application of a nitrogen flow at 15 psi for 1 h.

The above capillaries were sealed at both ends and heated in an oven at 70°C for 24 h to complete the polymerization reaction. Finally, the completed capillaries were washed successively with H_2O, 1-propanol, and acetone for 30 min each and then ready for the CEC experiments.

2.4 CEC experiments

The optimum BGE were borate and phosphate buffers for the present samples and columns, although several typical buffers, for example, citrate, acetate, and Tris, have been used previously. DMSO was used as the neutral marker. At the end of the analysis, the BMA-MES capillary was washed sequentially with MeOH, pure water, and running buffer during the intervals between runs. Prior to sample injection, a working voltage was applied for 5 min to condition the charge distribution in the column. The samples were then injected *via* height difference siphoning. Samples were detected by UV light absorption at 214 or 280 nm. All CEC experiments were conducted at room temperature.

3 Results and discussion

3.1 Measurements of EOF and SEM for the modified capillaries

The six curves shown in Fig. 1 illustrate the pH dependence of the EOF behavior of the bare capillary and of the capillaries obtained from the further silanization and polymerization steps. The curves for a bare fused silica, the silanized, the BMA-MES, and the BMA-CNT capillaries were adapted from previous results [33, 37]. Through silanization with the γ-MAPS reagent, the silanol groups on the silica surface of a bare capillary were converted to the unionizable bridging acrylate ligands ready for subsequent free radical polymerizations with various acrylate monomers. However, this conversion rate was only 20%, *i.e.* nearly 80% of the free silanol groups were still present in the capillary after silanization. The contribution of the unreacted silanol residues to the EOF could, therefore, continue to affect the BMA-MES and the MES-EDMA capillaries. Therefore, these two capillaries contained ionizable groups of residual silanol and MES molecules and thus had higher μ_{eo} values than the γ-MAPS-silanized capillary with only free silanols. Under the influence of the silanol residues, the EOF curve patterns for the BMA-MES and MES-EDMA capillaries would look like that for the bare capillary. After closely checking the two curves, an apparently upward trend of the μ_{eo} values appeared around pH 4.5 and 4.0 for the BMA-MES and the MES-EDMA capillaries, respectively, while the succinyl acid group in the MES molecular structure has a pK_a value of 4.0.

As shown in Fig. 1, the upper curve is the apparent depiction of μ_{eo} performance for the BMA-MES capillary and the lower curve is for the MES-EDMA capillary. If the silanol contribution to the EOF for the two capillaries was equivalent, the loading amount of the MES moiety for the BMA-MES capillary should be higher than the MES-EDMA

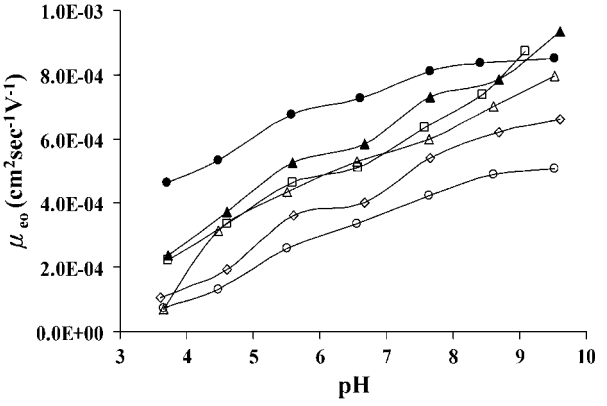

Figure 1. Dependence of electroosmotic mobility on buffer pH. Columns: (□) bare fused silica capillary; (◇) γ-MAPS-silanized capillary; (▲) BMA-MES capillary; (△) MES-EDMA capillary; (●) BMA-CNT capillary; (○) MES-CNT capillary. Conditions: BGE, phosphate buffer, 50 mM; sample, DMSO; hydrostatic injection, 5 cm, 2 s; applied voltage, 15 kV; detection, 214 nm.

capillary. Under SEM analysis, however, no trace of polymer materials was found in the MES-EDMA capillary after either leaving a thin layer of the MES monomeric solution or complete filling of this solution for reaction with the γ-MAPS-silanized capillary. When using the full-filling method, however, the entire BMA-MES column was plugged with the acrylate copolymers. This observation meant that the reactivity between the BMA monomers was much higher than that between the MES monomers, *i.e.* the formation of a BMA polymer was easier than a MES polymer. Furthermore, the γ-MAPS molecules fixed on the silanized capillary reacted with the MES monomers and formed a monolayered phase, which held fewer MES ligands in the completed MES-EDMA capillary in comparison with the polymeric phase formed in the BMA-MES capillary. This morphological state was quite similar to a SiH-MES capillary, where a MES monolayer was covalently bonded to the unionizable silica hydride surface (SiH) with only a few free silanols remaining [38].

The curves that correlated with the BMA-CNT and the MES-CNT capillaries did not follow the pattern of a bare capillary, as did the BMA-MES and the MES-EDMA capillaries. Instead of an obvious increase in μ_{eo} values around pH 6.8, the curves for the two CNT-related capillaries rose smoothly with increasing pH levels and seemed to reach a certain maximum μ_{eo} above pH 8.5. Here, the unreacted silanols could be somewhat shielded by the polymeric composites of the CNT materials. With a long, stick-like structure, the CNT rod might lie down in the non-silanized area and then develop bonding with BMA or MES monomers. Thus, the silanols would be beneath the CNT composites and would have limited impact on the EOF performance. Thus, the carboxylate groups in the structure of the acid-treated CNTs created the most surface charges and exerted the most EOF observed in the CNT-related capillaries.

As shown in Fig. 1, the EOF driven in the MES-CNT phase was much slower than that of the BMA-CNT capillary and even lower than with the γ-MAPS-silanized capillary. Besides the unreacted silanols, most of the CNT moieties should be blocked by the formation of the MES-CNT phase. The SEM images of the MES-CNT capillary, as shown in Fig. 2A and B, displayed few traces of CNT materials exposed on the porous surface layers but rather mostly embedded in the MES polymer. When the monomeric solution prepared for the formation of the MES-CNT capillary was polymerized on a sheet of aluminum foil, the SEM image of the resulting bulk materials showed the embedment of CNTs (Fig. 2C). Here, the MES-CNT phase exhibited a ''flexibility'' when compared to the BMA-CNT phase in Fig. 2D. This image also showed that some parts of the phase were collapsed by the cutting force applied to the capillary for the SEM sample preparation, revealing the fragility of the composite. It was suggested, therefore, that the BMA component is a ''hard'' CNT-binder while the MES component is a relatively ''soft'' binder.

The reproducibility of capillary fabrication was evaluated from the μ_{eo} values, which were measured from the migration times of neutral marker, DMSO, at pH 7.6 for five runs in a capillary using the same format. The RSD values were 3.5, 4.4, and 4.7% for three replicate MES-EDMA capillaries and 3.7, 4.1, and 4.6% for the MES-CNT capillaries. At the 95% confidence level, no significant difference in μ_{eo} values between capillaries was observed by *t*-test. The assessments of the BMA-MES and BMA-CNT capillaries were carried out in last reports [33, 37]. The four capillaries could be used for

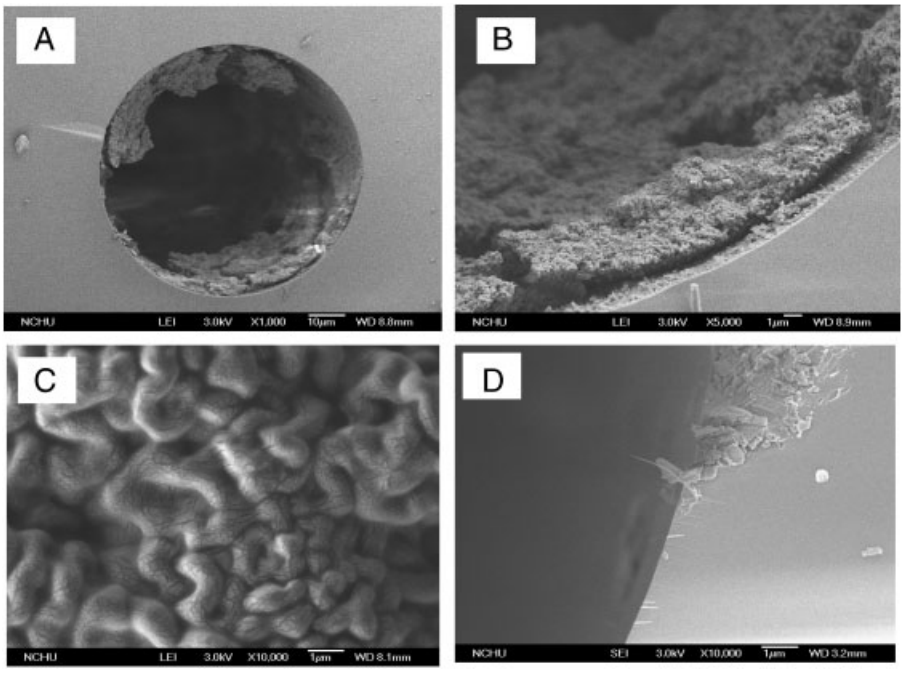

Figure 2. SEM images of prepared CNTs-polymer composites. (A) The MES-CNT coated on capillary wall; (B) five-fold magnification of (A); (C) the MES-CNT formed on aluminum foil; (D) the BMA-CNT coated on capillary wall. Figure 2D is cited from reference [37].

more than 200 times in half a year in the studies on the separations of flavonoids and phenolic acids under various running buffers across wide pH ranges (pH 2–10) and volume ratios of organic modifier (5–100%). This indicated the fabrication of the modified capillaries was pretty robust.

3.2 Comparison of the MES-EDMA capillary with the BMA-MES capillary

In a previous study, flavonoids and phenolic acids were successfully separated on a BMA-MES capillary [33]. To investigate the role of BMA in the separations, the newly synthesized MES-EDMA capillary, whose preparation was identical to that of the BMA-MES capillary except for the lack of BMA monomers in the polymerization solution, was compared to the BMA-MES capillary in CEC performance. The same analytes and running buffer conditions were used so the comparison could be focused on the difference between the two bound phases.

Owing to the fact that EOF varied with the capillaries (Fig. 1), the capacity factor observed from the electrochromatograms should be corrected by this variable. Rathore and Horváth suggested the measurement of the CEC mechanism from the contributions of the electrophoretic migration and the chromatographic retention, which were displayed as a velocity factor (k_e) and a retention factor (k''), respectively [39, 40]. Briefly, they are expressed by Eqs. (1) and (2):

$$k_e = \frac{\mu_{ep}}{\mu_{eo2}} \quad (1)$$

$$k'' = \frac{t_{M2} \times (1+k_e) - t_{02}}{t_{02}} \quad (2)$$

where μ_{ep} and μ_{eo2} are the electrophoretic and electroosmotic mobility, respectively. These values can then be obtained from OT-CE experiments on a bare capillary (column 1) and from CEC experiments on a CEC capillary (column 2), respectively, as follows:

$$\mu_{ep} = \mu - \mu_{eo1} = \frac{L_1 \times L_{d1}}{V_1} \times \left(\frac{1}{t_{M1}} - \frac{1}{t_{01}}\right)$$

$$\mu_{eo2} = \frac{L_2 \times L_{d2}}{t_{02} \times V_2}$$

where μ is the overall mobility of the analyte migrating in column 1, μ_{eo1} is the electroosmotic mobility for a neutral marker migrating in column 1, L is the total column length, L_d is the distance between the inlet and the detection point, V is the applied voltage, t_M is the migration time of solute, and t_0 is the migration time of the neutral marker.

3.2.1 Separation of flavonoids

Based on the same running buffer, a comparison between bare fused silica, BMA-MES and MES-EDMA capillaries would be useful for determining the effect of BMA in the bound phase. Although the optimum buffer conditions for the BMA-MES capillary were selected as the running buffer here, they were not optimal for the other capillaries. The electrochromatograms demonstrating the influence of different capillaries on the separation of these flavonoids in a borate buffer (pH 9.5, 10 mM) with MeOH modifier (30%, v/v) are given in Fig. 3. As shown in the electrochromatograms, the migration order of naringin and epicatechin in the bare fused silica capillary were different from those in the BMA-MES and MES-EDMA capillaries. Furthermore, the migration times of all the flavonoids in the MES-EDMA capillary were much shorter than in the BMA-MES capillary, even though the EOF exerted from the MES-EDMA phase was slower than the BMA-MES phase (Fig. 2). Therefore, the strength of the chromatographic retention of flavonoids in the MES-EDMA capillary must have been less than in the BMA-MES. The extent of this retention could be measured as the retention factor (k'').

For comparison, the electrochromatographic parameters of the flavonoids observed in Fig. 3 are listed in Table 1. The k'' values presented in the MES-EDMA capillary were all negative, which meant the nature of the chromatographic retention between the flavonoids and the MES-EDMA phase was repulsive. Electrostatic repulsion might have occurred between the anionic solutes and the succinate groups dissociated from the MES ligands in the wall coatings, as the pK_a value of succinyl acid (4.0) and of

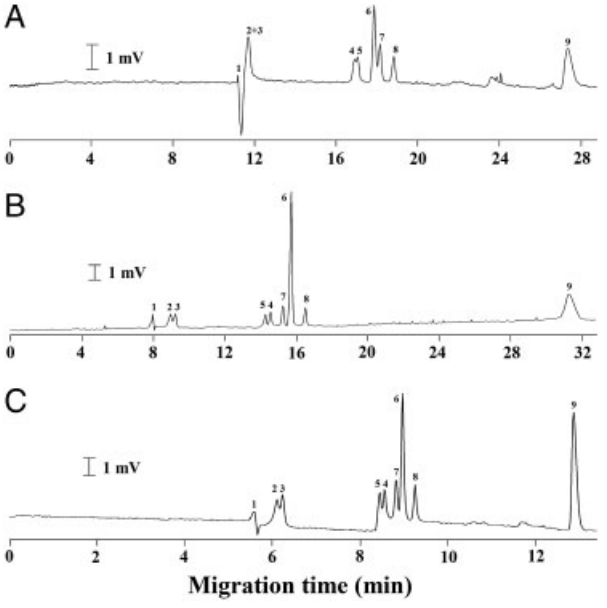

Figure 3. Electrochromatographic separations of flavonoids in various capillaries. (A) Bare fused silica (60 cm (55 cm) × 75 μm id); (B) BMA-MES (44 cm (39 cm) × 75 μm id); (C) MES-EDMA (45 cm (40 cm) × 75 μm id) in 10 mM borate buffer, pH 9.5, with 30% v/v MeOH. Samples: 0.25 mg/mL in MeOH; hydrostatic injection, 15 cm, 15 s; detection, 280 nm. Applied voltage: 15 kV. Peak identification: (1) 5-methoxyflavone, (2) hesperidin, (3) naringin, (4) epicatechin, (5) catechin, (6) hesperetin, (7) daidzein, (8) naringenin, and (9) quercetin.

Table 1. Electrochromatographic parameters of the flavonoids and phenolic acids separated in the BMA-MES and the MES-EDMA columns

Compounds	Bare fused-silica column		Compounds	BMA-MES column			Compounds	MES-EDMA column		
	t_{M1} (min)	$\mu_{ep} \times 10^{-4}$ (cm^2/s V)		t_{M2} (min)	k_e	k''		t_{M2} (min)	k_e	k''
Flavonoids separated in CEC conditions identical to those used in Fig. 3										
5-Methoxyflavone	6.915	0.3	5-Methoxyflavone	7.909	0.07	0.78	5-Methoxyflavone	5.558	0.08	−0.06
Hesperidin	8.712	−0.4	Hesperidin	8.902	−0.10	0.70	Hesperidin	6.085	−0.12	−0.17
Naringin	8.966	−0.5	Naringin	9.174	−0.11	0.71	Naringin	6.197	−0.15	−0.17
Epicatechin	12.445	−1.1	Catechin	14.208	−0.29	1.12	Catechin	8.425	−0.37	−0.17
Catechin	12.698	−1.2	Epicatechin	14.499	−0.28	1.19	Epicatechin	8.537	−0.36	−0.15
Hesperetin	12.953	−1.2	Hesperetin	15.198	−0.30	1.24	Hesperetin	8.8	−0.38	−0.15
Daidzein	13.585	−1.3	Daidzein	15.662	−0.32	1.25	Daidzein	8.944	−0.41	−0.17
Naringenin	16.341	−1.6	Naringenin	16.453	−0.39	1.12	Naringenin	9.23	−0.49	−0.27
Quercetin	22.433	−1.9	Quercetin	31.208	−0.48	2.44	Quercetin	12.847	−0.61	−0.21
Phenolic acids separated in CEC conditions identical to those used in Fig. 4										
Ethylvanillin	4.563	−2.6	Ethylvanillin	3.225	−0.35	0.35	Ethylvanillin	4.208	−0.45	−0.14
Chlorogenic acid	8.142	−4.7	Chlorogenic acid	5.612	−0.63	0.33	Chlorogenic acid	5.966	−0.82	−0.60
Syringic acid	10.072	−5.2	Ferulic acid	8.855	−0.70	0.71	Ferulic acid	7.662	−0.91	−0.74
Ferulic acid	10.107	−5.3	Syringic acid	9.458	−0.70	0.83	Syringic acid	7.963	−0.91	−0.72
Vanillic acid	10.533	−5.3	Gallic acid	10.412	−0.80	0.35	Protocatechuic acid	9.103	−1.10	−1.34
p-Coumaric acid	11.68	−5.5	*p*-Coumaric acid	11.689	−0.74	0.96	Vanillic acid	9.561	−0.92	−0.73
p-Hydroxybenzoic acid	14.309	−5.9	*p*-Hydroxybenzoic	12.687	−0.79	0.76	Gallic acid	10.565	−1.04	−1.14
Gallic acid	15.3	−6.0	Protocatechuic acid	15.779	−0.85	0.54	*p*-Coumaric acid	11.385	−0.96	−0.83
Protocatechuic acid	20.742	−6.4	Vanillic acid	19.663	−0.71	2.64	*p*-Hydroxybenzoic acid	12.128	−1.02	−1.08

the flavonoids (ranging from 6.8 to 8.2) were below the pH 9.5 of the borate buffer used [41]. Although hesperidin and naringin have higher pK_a values (10.0 and 10.2, respectively) than 9.5, they might have formed anionic complexes *via* the equilibrium between the borate ions and the diol groups of the glucoside moieties in their structures [42]. As a result, these anionic solutes migrated toward the anode and had negative μ_{ep} or k_e values for all three capillaries listed in Table 1.

In contrast with the MES-EDMA capillary, the BMA-MES capillary had positive k'' values and, thus, had longer migration times for the analytes. It was believed that the presence of BMA in the polymer phase could not only help to form thicker porous coatings, but also afford stronger hydrophobic interactions with the flavonoid solutes and higher selectivities between them.

Tiny differences in the skeleton or substituent position of the flavonoid compounds might cause diverse retention times on the BMA matrix phase in a reversed-phase LC mode [43]. In the CEC, the addition of MeOH into the running buffer affected the chromatographic partitioning and also altered the EOF. Moreover, the k'' and k_e values were generally parallel to the migration order. That is, the electrophoretic and chromatographic modes collectively determined the CEC mechanism in the BMA-MES capillary. Unlike those for the BMA-MES capillary, most of the k'' values for the MES-EDMA capillary did not follow the trend that lower k'' values led to higher the migration order. Accordingly, the order of analytes was mainly determined by electrophoresis, not by chromatography. In addition, the difference between the k'' values was not large enough to sustain a sufficient selectivity of the flavonoids in the buffer conditions and thus, resulted in a poor resolution (Fig. 3C).

3.2.2 Separation of phenolic acids

In comparison with the flavonoids, phenolic acids are fully ionized in a general buffer with a moderate pH level. With pK_a values ranging between 3.59 and 4.64, the eight phenolic acids selected were all from plants, such as yacón leaves [44] and *Acanthopanax senticosus* roots [45]. The acids were mixed with ethylvanillin, pK_a = 7.6, and used to test the CEC performance in the BMA-MES capillary. With the aid of the cathodic EOF generated by a voltage of +20 kV, the elution of the acids could be achieved within 21 min using the BMA-MES capillary in 50 mM phosphate buffer at pH 6.6, as shown in Fig. 4B. This electrochromatogram showed a better resolution and shorter analysis time than that recorded for a bare fused silica capillary (Fig. 4A). As can be seen in Fig. 4C, the MES-EDMA capillary had the shortest migration times for phenolic acids. It is worth noting that the migration orders for the three capillaries were totally different from each other. In addition to zone electrophoresis, the chromatographic retention of the acids should play an important role in CEC separations.

The electrochromatographic parameters corresponding to the separations in Fig. 4 are listed in Table 1. The satisfactory selectivity arising from the BMA-MES capillary primarily originated from the different k'' factors, which ranged from 0.33 to 0.96. The k_e factors, for comparison,

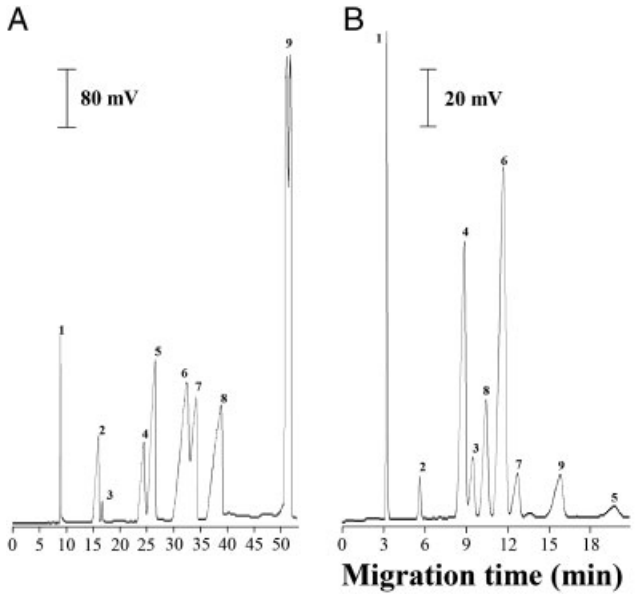

Figure 4. Electrochromatographic separations of phenolic acids in various capillaries. (A) Bare fused silica (60 cm (55 cm) × 75 μm id); (B) BMA-MES (40 cm (35 cm) × 75 μm id); (C) MES-EDMA (46 cm (41 cm) × 75 μm id) in 50 mM phosphate buffer, pH 6.6. Samples: 0.1 M in H_2O; hydrostatic injection, 15 cm, 5 s; detection, 214 nm. Applied voltage: 20 kV. Peak identification: (1) ethylvanillin, (2) chlorogenic acid, (3) syringic acid, (4) ferulic acid, (5) vanillic acid, (6) *p*-coumaric acid, (7) *p*-hydroxybenzoic acid, (8) gallic acid, and (9) protocatechuic acid.

were only within a narrow range from −0.63 to −0.85. In comparison with the k_e factors, ranging from −0.82 to −1.10, the k'' factors with a wider range from −0.60 to −1.34 also dominated the selectivity of the MES-EDMA capillary. In this capillary, the negative k'' values were reflective of the repulsion between the phenolic carboxylates and the MES-EDMA phase, but did not correlate with the migration order. These observations were similar to those seen for the flavonoids. However, phenolic acids possess more negative μ_{ep} values than flavonoids, as shown in the bare fused silica column in Table 1. This property makes the k_e and k'' values corresponding to the phenolic acids smaller in either the BMA-MES capillary or in the MES-EDMA capillary compared to flavonoids. While this decrease occurred in the BMA-MES capillary, the BMA-based matrix itself could afford a certain amount of interaction with the phenolic solutes and still keep the k'' values positive. Nevertheless, the values of k'' were less closely related to the migration order than k_e, and thus the electrophoresis factor seemed to be the main determinant of the migration order.

3.3 Comparison of the MES-CNT capillary with the BMA-CNT capillary

According to the above SEM observations, the role of the BMA in the BMA-CNT phase could be regarded as a CNT binder, rather than a bulk monomer, while the affinity for self-polymerization of BMA monomers was too strong to create a homogeneous phase. On the contrary, the MES compound could be a good bulk monomer to co-polymerize with the acidified CNTs and to form a composite phase with a well-distributed roughness. The two capillaries with different phase morphologies were compared by their CEC performance on the flavonoid and phenolic acid samples, and the running buffer conditions used for the BMA-CNT capillary were identical to those used in the previous study [37].

3.3.1 Separation of flavonoids

The electrochromatograms demonstrating the influence of the capillaries, including a bare fused silica, the BMA-CNT, and the MES-CNT capillaries, on the separation of the selected flavonoids in borate buffer (pH 9.5, 10 mM) with ACN modifier (50%, v/v) are given in Fig. 5. For the bare capillary, where the CEC conditions used a lower electrical field and a higher modifier ratio than those in Fig. 3A, the increased migration times and improved peak resolutions are shown in Fig. 5A. However, an irreversible adsorption on the bare capillary caused the short peak heights and some unidentified peaks. Compared to Fig. 5A, the figures in Fig. 5B and C, corresponding to the BMA-CNT and the MES-CNT capillaries, show higher intensities of the sample peaks with acceptable resolutions.

The electrochromatographic parameters corresponding to the separations in Fig. 5 are listed in Table 2. As the data show, the k'' values obtained from the BMA-CNT capillary were higher than those from the MES-CNT capillary. One reason for this phenomenon was based on the higher hydrophobicity of the BMA units in the BMA-CNT phase than the MES units in the MES-CNT phase. Another reason was that the immobilized CNTs, which exert stronger π–π interactions with the benzyl rings in the flavonoid structures, had a smaller surface contact area in the MES-CNT phase than in the BMA-CNT phase. The contribution from the immobilized CNTs to the k'' values could then be roughly estimated by comparison of the k'' values of the MES-EDMA capillary listed in Table 1 with the MES-CNT capillary listed in Table 2. The observed increases in the k'' values ranged from 0.01 for 5-methoxylflavone to 2.36 for quercetin. These increases would have been larger, however,

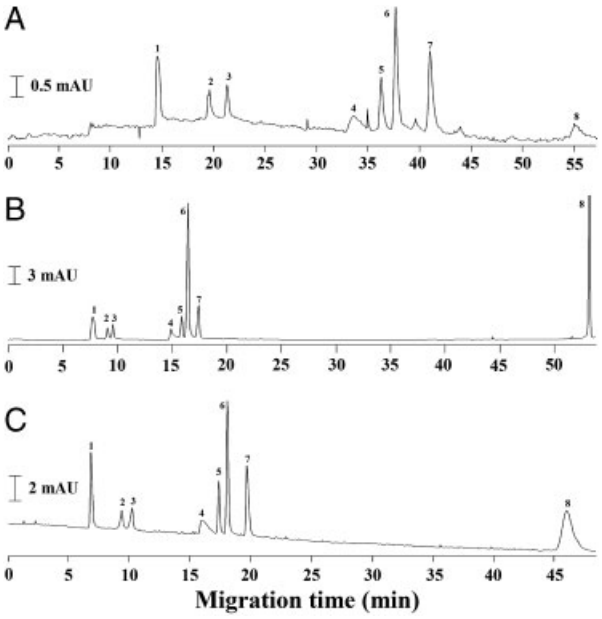

Figure 5. Electrochromatographic separations of flavonoids in various capillaries. (A) Bare fused silica (53 cm (48 cm) × 75 μm id); (B) BMA-CNT (38 cm (33 cm) × 75 μm id); (C) MES-CNT (41 cm (36 cm) × 75 μm id) in 10 mM borate buffer, pH 9.5, with 50% v/v ACN. Samples: 0.25 mg/mL in MeOH; hydrostatic injection, 15 cm, 15 s; detection, 280 nm. Applied voltage: 10 kV. Peak identification: (1) 5-methoxyflavone, (2) hesperidin, (3) naringin, (4) epicatechin, (5) hesperetin, (6) daidzein, (7) naringenin, and (8) quercetin.

except that a higher volume of organic modifier was used in the MES-CNT capillary (50% ACN) than in the MES-EDMA capillary (30% MeOH). If the increases in k'' values were analogous to the contribution from the incorporated CNTs in the BMA-CNT phase, this contribution would be around 44–66%, *i.e.* nearly half of the flavonoids were retained by the BMA and the other half by CNTs.

In Table 2, both the k_e and k'' values were generally parallel to the migration order in the BMA-CNT and MES-CNT capillaries, *i.e.* the electrophoretic and chromatographic modes determined the CEC mechanism cooperatively. In contrast to the MES-EDMA capillary, whose separation mechanism was mainly determined by electrophoresis, the CNTs moieties attached in the MES-CNT capillary actually boosted the chromatographic retention of the flavonoids. Although the carboxylate groups in the acid-treated CNTs could provide hydrogen-bonding sites, they did not seem to be a crucial factor, as the many hydroxyl groups in the hesperidin and naringin structures did not significantly raise their k'' values in the two CNT-related capillaries.

3.3.2 Separation of phenolic acids

Figure 6 illustrates the electrochromatograms for the phenolic acids separated in borate buffer (pH 9.5, 30 mM) with MeOH modifier (10%, v/v) by a bare fused silica, the BMA-CNT, and the MES-CNT capillaries. The CEC parameters corresponding to these separations are listed in

Table 2. Electrochromatographic parameters of the flavonoids and phenolic acids separated in the BMA-CNT and the MES-CNT columns

Compounds	Bare fused-silica column		Compounds	BMA-CNT column			Compounds	MES-CNT column		
	t_{M1} (min)	$\mu_{ep} \times 10^{-4}$ (cm^2/s V)		t_{M2} (min)	k_e	k''		t_{M2} (min)	k_e	K''
Flavonoids separated in CEC conditions identical to those used in Fig. 5										
5-Methoxyflavone	9.242	−0.19	5-Methoxyflavone	7.636	−0.04	0.53	5-Methoxyflavone	6.747	−0.05	−0.05
Naringin	9.644	−0.28	Hesperidin	8.969	−0.11	0.68	Hesperidin	9.291	−0.12	0.21
Hesperidin	10.438	−0.45	Naringin	9.474	−0.07	0.85	Naringin	10.143	−0.08	0.39
Epicatechin	24.124	−1.6	Epicatechin	14.765	−0.38	0.93	Epicatechin	15.86	−0.44	0.32
Daidzein	32.657	−1.9	Hesperetin	15.743	−0.45	0.81	Hesperetin	17.272	−0.53	0.21
Hesperetin	38.352	−1.9	Daidzein	16.334	−0.43	0.95	Daidzein	17.987	−0.50	0.33
Quercetin	41.263	−2.0	Naringenin	17.283	−0.46	0.94	Naringenin	19.585	−0.54	0.34
Naringenin	41.991	−2.0	Quercetin	52.892	−0.46	4.96	Quercetin	45.921	−0.54	2.15
Phenolic acids separated in CEC conditions identical to those used in Fig. 6										
Ethylvanillin	2.678	−5.7	Ethylvanillin	14.71	−0.43	1.31	Ethylvanillin	19.688	−0.73	0.15
Chlorogenic acid	2.698	−5.8	Chlorogenic acid	18.034	−0.58	1.80	Chlorogenic acid	23.822	−0.74	0.37
Ferulic acid	2.997	−6.3	Ferulic acid	19.873	−0.64	1.69	Syringic acid	24.872	−0.81	0.04
Syringic acid	3.01	−6.3	Syringic acid	20.795	−0.64	1.80	Ferulic acid	25.905	−0.81	0.10
p-Coumaric acid	3.241	−6.7	*p*-Coumaric acid	24.49	−0.67	1.98	*p*-Coumaric acid	29.806	−0.85	−0.04
Vanillic acid	3.45	−6.9	Vanillic acid	25.446	−0.70	1.84	Vanillic acid	30.973	−0.89	−0.24
p-Hydroxybenzoic acid	4.01	−7.5	*p*-Hydroxybenzoic acid	32.858	−0.76	1.95	*p*-Hydroxybenzoic acid	38.422	−0.96	−0.69
Caffeic acid	5.456	−8.5	Caffeic acid	38.779	−0.85	1.10	Caffeic acid	47.212	−1.09	−1.88
Protocatechuic acid	6.027	−8.7	Gallic acid	44.857	−0.92	0.41	Gallic acid	53.018	−1.16	−2.90
Gallic acid	7.083	−9.1	Protocatechuic acid	62.498	−0.88	1.80	Protocatechuic acid	69.323	−1.12	−2.79

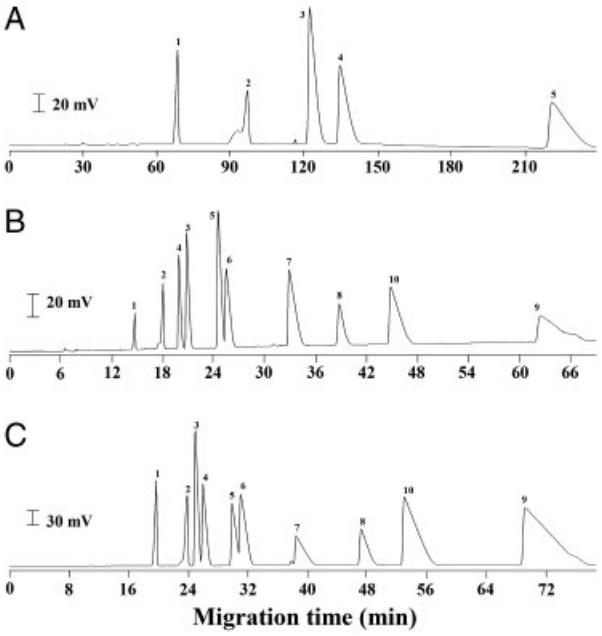

Figure 6. Electrochromatographic separations of phenolic acids in various capillaries. (A) bare fused silica (44 cm (39 cm) × 75 μm id); (B) BMA-CNT (36 cm (31 cm) × 75 μm id); (C) MES-CNT (41 cm (36 cm) × 75 μm id) in 30 mM borate buffer, pH 9.5, with 10% v/v MeOH. Samples: 0.1 M in H_2O; hydrostatic injection, 15 cm, 1 s; detection, 214 nm. Applied voltage: 7 kV. Peak identification: (1) ethylvanillin, (2) chlorogenic acid, (3) syringic acid, (4) ferulic acid, (5) *p*-coumaric acid, (6) vanillic acid, (7) *p*-hydroxybenzoic acid, (8) caffeic acid, (9) protocatechuic acid, and (10) gallic acid.

Table 2. By comparison of the bare fused silica capillary data in Table 1 and 2, the phenolic acids had more negative μ_{ep} values in the buffer conditions of Fig. 6 than those in Fig. 4. As a result, in addition to a lower electric field applied in the conditions of Fig. 6, the migration times shown in Fig. 6A were much larger than those in Fig. 4A. Furthermore, the migration orders for the two CNT-related capillaries, as shown in Fig. 6B and C, were much more parallel to those of a bare capillary than the BMA-MES and the MES-EDMA capillaries, which are presented in Fig. 4. With high negative μ_{ep} values, these acid analytes separated in the conditions of Fig. 6 suggested the CEC mechanism was dominated by electrophoresis, as the strong electrostatic repulsion between negatively charged solutes and phase surfaces prevented chromatographic retention.

As shown in Table 2, the k'' values observed in the BMA-CNT capillary were larger than those in the MES-CNT capillary. This observation was similar to that for flavonoids and was discussed in Section 3.2.1. However, a decrease in k'' values was disclosed in the separation of the phenolic acids with the MES-CNT capillary. Here, the acid solutes with negative μ_{ep} values experienced an extra repulsive interaction with the MES-CNT phase, which had no hydrophobic BMA units and few CNT moieties exposed on the contact surface.

4 Concluding remarks

Two new synthetic stationary phases, MES-EDMA and MES-CNT, were designed to probe the function of the bulk monomer BMA in the BMA-MES and BMA-CNT phases of capillaries used in our previous research. The pH-dependent EOF performances of the two new phases were reasonably comparable with the two previous phases and were comparable to their SEM images. In a comparison of BMA-MES and MES-EDMA capillaries, BMA was found to help form a thicker BMA-MES polymer phase, which then held more bonding linkages with ionizable MES ligands and afforded stronger non-polar interactions with the flavonoids and phenolic acids than a simple MES-EDMA phase. As compared with the two CNT-related capillaries, BMA also functioned as a CNT-binder and constructed the inhomogeneous BMA-CNT phase, where isolated CNTs afforded more π–π interactions with the analytes than the CNTs bound to the MES monomer and embedded in the MES-CNT phase. A further determination of the chromatographic interactions arising from the above CEC phases will be discussed in terms of solvation parameter models in the near future.

Support of this work by the National Science Council of Taiwan (NSC-96-2113-M-039-004-MY2 and NSC-98-2113-M-039-003-MY3) and by the China Medical University (CMU99-S-48) is gratefully acknowledged.

The authors have declared no conflict of interest.

5 References

[1] Hjertén, S., Liao, J.-L., Zhang, R., *J. Chromatogr.* 1989, *473*, 273–275.

[2] Ou, J., Dong, J., Dong, X., Yu, Z., Ye, M., Zou, H., *Electrophoresis* 2007, *28*, 148–163.

[3] Wu, R., Hu, L., Wang, F., Ye, M., Zou, H., *J. Chromatogr. A* 2008, *1184*, 369–392.

[4] Smith, N. W., Jiang, Z., *J. Chromatogr. A* 2008, *1184*, 416–440.

[5] Dong, X., Wu, R., Dong, J., Wu, M., Zhu, Y., Zou, H., *Electrophoresis* 2009, *30*, 141–154.

[6] Eeltink, S., Svec, F., *Electrophoresis* 2007, *28*, 137–147.

[7] Huang, Y.-P., Liu, Z.-S., Zheng, C., Gao, R.-Y., *Electrophoresis* 2009, *30*, 155–162.

[8] Peters, E. C., Petro, M., Svec, F., Frechet, J. M. J., *Anal. Chem.* 1998, *70*, 2288–2295.

[9] Cantó-Mirapeix, A., Herrero-Martínez, J. M., Mongay-Fernández, C., Simó-Alfonso, E. F., *Electrophoresis* 2008, *29*, 3866–3874.

[10] Karenga, S., El Rassi, Z., *J. Sep. Sci.* 2008, *31*, 2677–2685.

[11] Cantó-Mirapeix, A., Herrero-Martínez, J. M., Mongay-Fernández, C., Simó-Alfonso, E. F., *Electrophoresis* 2009, *30*, 607–615.

[12] Lu, M., Feng, Q., Lu, Q., Cai, Z., Zhang, L., Chen, G., *Electrophoresis* 2009, *30*, 3540–3547.

[13] Bisjak, C. P., Trojer, L., Lubbad, S. H., Wieder, W., Bonna, G. K., *J. Chromatogr. A* 2007, *1154*, 269–276.

[14] Cantó-Mirapeix, A., Herrero-Martínez, J. M., Baeza-Baeza, J. J., Simó-Alfonso, E. F., *J. Chromatogr. A* 2009, *1216*, 6831–6837.

[15] Barrioulet, M.-P., Delaunay-Bertoncini, N., Demesmay, C., Rocca, J.-L., *Electrophoresis* 2005, *26*, 4104–4115.

[16] Cantó-Mirapeix, A., Herrero-Martínez, J. M., Mongay-Fernández, C., Simó-Alfonso, E. F., *Electrophoresis* 2009, *30*, 599–606.

[17] Wang, J., Lu, H., Lin, X., Xie, Z., *Electrophoresis* 2008, *29*, 928–935.

[18] Fu, H., Xie, C., Xiao, H., Dong, J., Hu, J., Zou, H., *J. Chromatogr. A* 2004, *1044*, 237–244.

[19] Lämmerhofer, M., Svec, F., Fréchet, J. M. J., Lindner, W., *J. Microcolumn Sep.* 2000, *12*, 597–602.

[20] Viklund, C., Irgum, K., *Macromolecules* 2000, *33*, 2539–2544.

[21] Kapnissi-Christodoulou, C. P., Zhu, X., Warner, I. M., *Electrophoresis* 2003, *24*, 3917–3934.

[22] Guihen, E., Glennon, J. D., *J. Chromatogr. A* 2004, *1044*, 67–81.

[23] Huang, X., Zhang, J., *Horváth, Cs. J. Chromatogr. A* 1999, *858*, 91–101.

[24] Chuang, S.-C., Chang, C.-Y., Liu, C.-Y., *J. Chromatogr. A* 2004, *1044*, 229–236.

[25] Tan, Z. J., Remcho, V. T., *Anal. Chem.* 1997, *69*, 581–586.

[26] Huang, T., Mi, J.-Q., Zhang, X.-X., *J. Sep. Sci.* 2006, *29*, 277–281.

[27] Eeltink, S., Svec, F., Fréchet, J. M. J., *Electrophoresis* 2006, *27*, 4249–4256.

[28] Xu, L., Sun, Y., *Electrophoresis* 2007, *28*, 1658–1667.

[29] Xu, L., Sun, Y., *Electrophoresis* 2008, *29*, 880–888.

[30] Xu, L., Sun, Y., *J. Chromatogr. A* 2008, *1183*, 129–134.

[31] Zaidi, S. A., Cheong, W. J., *J. Chromatogr. A* 2009, *1216*, 2947–2952.

[32] Xu, L., Dong, X.-Y., Sun, Y., *Electrophoresis* 2009, *30*, 689–695.

[33] Chen, J.-L., Lin, Y.-C., *J. Chromatogr. A* 2010, *1217*, 4328–4336.

[34] Schmid, M. G., Koidl, J., Freigassner, C., Tahedl, S., Wojcik, L., Beesley, T., Armstrong, D. W., Gubitz, G., *Electrophoresis* 2004, *25*, 3195–3203.

[35] Schmid, M. G., Koidl, J., Wank, P., Kargl, G., Zöhrer, H., Gübitz, G., *J. Biochem. Biophys. Methods* 2007, *70*, 77–85.

[36] Choodum, A., Thavarungkul, P., Kanatharana, P., Smith, N. W., *Chromatographia* 2009, *69*, 481–488.

[37] Chen, J.-L., Lin, Y.-C., *Electrophoresis* 2010, *31*, 3217–3226.

[38] Chen, J.-L., *Electrophoresis* 2009, *30*, 3855–3862.

[39] Rathore, A. S., Horváth, Cs., *J. Chromatogr. A* 1996, *743*, 231–246.

[40] Rathore, A. S., Horváth, Cs., *Electrophoresis* 2002, *23*, 1211–1216.

[41] Chen, J.-L., *J. Chromatogr. A* 2010, *1216*, 6236–6244.

[42] Schmitt-Kopplin, Ph., Hertkorn, N., Garrison, A. W., Freitag, D., Kettrup, A., *Anal. Chem.* 1998, *70*, 3798–3808.

[43] Wang, S. P., Fu, M. D., Wang, M. H., *J. Chromatogr. A* 2007, *1164*, 306–312.

[44] Jirovský, D., Horáková, M., Kotoucek, M., Valentová, K., Ulrichová, J., *J. Sep. Sci.* 2003, *26*, 739–742.

[45] Zgórka, G., Kawka, S., *J. Pharm. Biomed. Anal.* 2001, *24*, 1065–1072.

